Novel Synthesis of Optical, Photoluminescence Properties and Supercapacitor Application on Zn^{2+} doping $Sn_{1-x}Zn_xO_2$ nanoparticles

S. Sivakumar[1*], E. Manikandan[1]

[1*]Dept. of Physics, Annamalai University, Annamalainagar-608 002, Tamil Nadu, India
[1]Department of physics, Annamalai University, Annamalainagar-608 002, Tamil Nadu, India

[1*]*Corresponding Author: girihari777@yahoo.com, mob: +91 - 9865043811*

Abstract - In this research on (0.00, 0.025, 0.045, 0.065 M %) Zn/SnO_2 nanoparticles have been prepared effectively chemical precipitation route on different doping concentration of zinc from 0.00 to 0.065%. XRD results showed the crystalline nature for different doping concentrations that are existed as a tetragonal structure. HR-TEM investigation of pictures confirms the presence of very little, homogeneously dispersed, and spherical shapes are observed. The crystallite size is calculated using the Scherrer formula and was formed in the size of nanoparticles range from 11.6 nm to 42.0 nm. The presence of dopant (i.e. Zn) and arrangement of Sn to O phase and hydrous nature of Zn/SnO_2 nanoparticles are confirmed by EDX and FTIR (O-Sn-O stretching) investigations. The band gap value is observed from 3.20 eV to 3.50 eV in undoped and Zn/SnO_2 nanoparticles, Due to the large grain size. The grains size develops so deformity density decreases and increases crystalllinity. These defects act as luminescent focuses and cause a decrease in emission intensity and increase in the band gap. The cyclic voltammetry investigation is a specific capacitance value, calculate as 496 F/g and 572 F/g was obtained at a scan rate 5 mV/s for undoped and (0.025 M %) Zn/SnO_2 nanoparticles it's suitable for supercapacitor applications.

Keywords: Zn/SnO_2 *nanoparticles, XRD, SEM, HR-TEM, UV-DRS, PL and CV.*

I. INTRODUCTION

It has been generally acknowledged in current years that electrochemical supercapacitors (ECs) are the most excellent possibility to give brilliant reversibility and high power density with a long cycle life for novel energy applications for example, burst power generation, memory back up devices with hybrid vehicles [1]. Therefore, the progress of proper electrode materials for ECs to gather the condition for high power and long durability is attracting in a lot thought. In view of the charge storage mechanism, electrochemical specific capacitance is separated into two types: (i) Electrical Double Layer Capacitors (EDLC) that use the capacitance emerging from charge separation an electrode/electrolyte interface and (ii) Pseudocapacitors that use the charge exchange emerging from redox responses happening the surface of an electrode. Pseudocapacitors are large generally examined on account of their high specific capacitance with high energy properties. Since, pseudocapacitance emerges from the redox reaction of electroactive materials, transition metal oxides [2, 3], and conductive polymers [4,5] with several oxidation states are considered promising electrode materials for pseudocapacitors. Transition metal oxides lectroactive materials. The anhydrous ruthenium oxide, metal oxides has higher capacitance with superb electrochemical reversibility [6]. SnO_2 nanoparticles used in potential gas sensing [7], dye sensing solar cells [8] and lithium-ion batteries [9]. It is well known that the regular ways to change the characteristics of a material is by introducing dopants into the structure. Doping with metal added substances (Al, Co, Fe and Cu) can prompt an increase in the surface region of SnO_2 based powders [10, 11], the balanced SnO_2 surface, and advance a decreased grain size. In case, the Zn dopant can reduce growth of crystallite and a main role in the electrochemical properties. The Sb doped SnO_2 nanocrystallites were prepared by sol-gel route and SC of 16 F/g got from a CV scan rate of 4 mV/s [12]. Similar authors have also studied the composite electrode of SnO_2 and RuO, and a specific capacitance value reported on 33 F/g of a scan rate 50 mV/s.

In this work, Zn/SnO_2 nanoparticles have been prepared chemical precipitation route for synthesizing Zn/SnO_2 nanoparticles that are nearing quantum confinement effect and its structural, optical and electrochemical properties are examined. For the best of our information, there are no reports in the literature about to the utilization of Zn/SnO_2 as electrode material for supercapacitor application.

II. MATERIALS AND METHOD

A. Materials

Sigma Aldrich AR grade purchased in all chemicals and used without any further purification. Aqueous solutions containing stoichiometries rates of the precursors for tin (IV) chloride pentahydrate ($SnCl_4.5H_2O$), Zinc (II) chloride hexahydrate ($ZnCl_2.6H_2O$) and distilled water were used in the followed synthesis process.

B. Synthesis of Zn/SnO$_2$ nanoparticles

All $Sn_{1-x}Zn_xO_2$ (x=0.00, 0.025, 0.045 and 0.065) samples were prepared by chemical precipitation route. For the synthesis of undoped and Zn/SnO$_2$, we have used two precursors as: (i) $SnCl_4. 5H_2O$ and $ZnCl_2.6H_2O$ (Precursor 1) and (ii) NH_4OH (Precursor 2). The precursor 1 is heated under constant stirring at 80^oC and Precursor 2 is added slowly, drop by drop in boiling Precursor 1 the solution is pH maintained at 9. Then the resulting solution was heated constantly for 2 hours until a White precipitate was formed which washed repeatedly with Distilled water and ethanol and dried at 100^oC. The as-prepared samples were annealed at 700^oC in a furnace under a continuous flow of O_2 and N_2 for 2hrs to obtain undoped and (0.025, 0.045, 0.065 M %) Zn/SnO$_2$ Samples, respectively.

C. Characterization of SnO$_2$ nanoparticles

The phase confirmation of the undoped and Zn/SnO$_2$ nanoparticles were characterized by PW3040/60 X pert PRO powder XRD with CuKα radiation (λ = 1.5406A$^\circ$) at 40 kV and 30 mA is using X-ray diffraction technique available at Alagappa university, Karaikudi. The scans for 2θ values in the angular range for 20° to 80° with 10°/min a scanning speed. JSM6701F MODEL using SEM with EDAX was well known utilizing a thermal emission electron microscope available in Manufacturing Engineering, Annamalai University, TN, India. JEM 2100 F MODEL using performed HR-TEM before conducting the examination, the products were sputtered. Morphological investigation used to size and shape available at SAIF, Cochin, Kerala, India. The SAED were confirmed in dispersion of the sample overa carbon coated copper grid. SHIMADZU-UV 2600 spectrometer using UV-Vis DRS available at dept. of Chemistry Annamalai University TN, India. Photoluminescence LS/55, Perkin Elmer and electrochemical property of the nanoparticles was performed by cyclic voltammetry model CHI 660 available at St. Joseph's college (autonomous), Thiruchirappalli, TN, India.

III. RESULT AND DISCUSSION

A. Phase Identification Analysis

  X- Ray Diffraction patterns are shown in Fig.1. It is clear that the position of the peak is agreed well with the reflection of rutile tetragonal structure of the SnO$_2$ phase (JCPDS#72-1147) in the all concentrations. Moreover, there is no additional peaks of the undoped and Zn/SnO$_2$ at 0.025 molar ratios wherein the diffraction peaks can accredit as (110), (101), (200), (111), (211), (220) plus (002) with no some additional phases detected indicating that the Zn ions be introduced by the crystal lattice of SnO$_2$. Moreover, the results indicate that Zinc ions obtain substituted at Sn site no changing the cassiterite structure. Notwithstanding, the secondary phase of the hexagonal is ZnO was distinguished at 0.045 and 0.065 Zn/SnO$_2$ nanoparticles molar ratio [13] (JCPDS#89-7102). It is watched peak position movements to higher 2θ as the ZnO molar ratio increments. Table 1 depicts the outlines difference in crystallite size and change in the lattice parameters were calculated from the peaks (110), (101) and (002) of Zn/SnO$_2$. The results were shown by the lattice parameters and the crystallite sizes were reduce with increasing Zn exchange ratio in table.1 [14]. As the concentration of doping increases, the intensity of the XRD peak decreases and the full width half maximum increases, because of the degradation of crystallinity. This suggests that even though Zn^{2+} ions occupy a normal Sn^{4+} lattice, it produces crystal defects about the dopants with charge imbalance emerging from this defect changes the stoichiometry of the materials. The lattice parameters for undoped and Zn/SnO$_2$ nanoparticles were predicted from the formula

$$\frac{1}{d_{hkl}^2} = \frac{h^2+k^2}{a^2} + \frac{l^2}{c^2} \qquad (1)$$

Where a and c are the lattice parameters, h, k, and l are the Miller indices, and d_{hkl} is interplanar spacing for the plane (hkl). This interplanar spacing is calculated by this formula

$$2d_{hkl}\sin\theta = n\lambda \qquad (2)$$

Where, x-ray wavelength is λ, the angle of Bragg diffraction is θ, and n is order of diffraction (n=1). The radius of ionic Sn^{4+} is 0.71 A$^\circ$, which is small, correlated to 0.74 A$^\circ$ for Zn^{2+} [15]. Because of this reality, the lattice

distortion could be credited to Zn^{2+} replacing Sn^{4+} in the lattice. Besides, the average crystallite size of the samples was calculated with Scherrer's formula

$$D = \frac{k\lambda}{\beta cos\theta}$$ (3)   [Ref 16]

Where D is the average crystallite size, β is the FWHM, λ is the x-ray wavelength (CuKα = 0.1546 nm), θ is the Bragg Diffraction angle, and k is a shape factor that is in use at 0.9. As Table 1 is depicted by the calculated value of the crystallite size is reduced from 42 nm to 11.6 nm among the increase in the (0.025, 0.045, 0.065 M %) concentration of Zn doping [17].
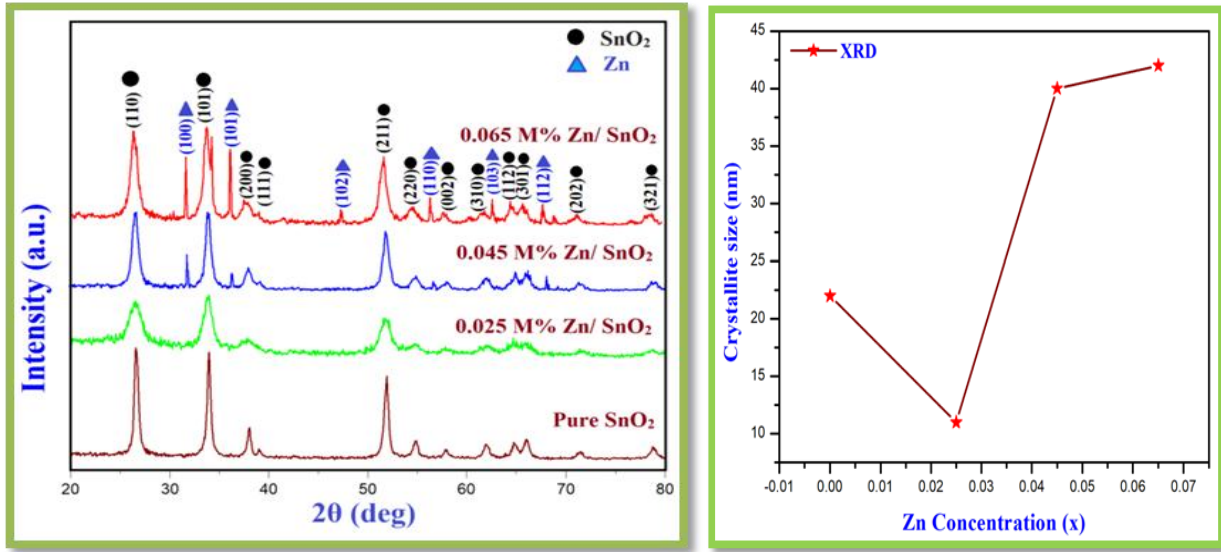

Figure 1. XRD patterns of Undoped and Zn/SnO₂ nanoparticles and Average crystallite size of the $Sn_{1-x}Zn_xO_2$ nanoparticles determined from XRD.

Table 1. Various structural and optical parameters of undoped and Zn/SnO₂ nanoparticles.

Samples	Lattice parameter a=b≠c (Tetragonal structure)		Average crystallite size (D) nm	Band gap Energy (eV)
	a=b	c		
Pure SnO₂	4.7308	3.1836	22.0	3.50
Zn 0.025%	4.7350	3.1942	11.6	3.38
Zn 0.045%	4.7444	3.1936	40.0	3.32
Zn 0.065%	4.7549	3.1907	42.0	3.20

B. Morphology Analysis

Scanning electron microscopy is most useful techniques for the utilization of nanostructures and nanomaterials. The signals that get from electron sample connections uncover information was concerned with the sample as including the surface morphology of the sample.
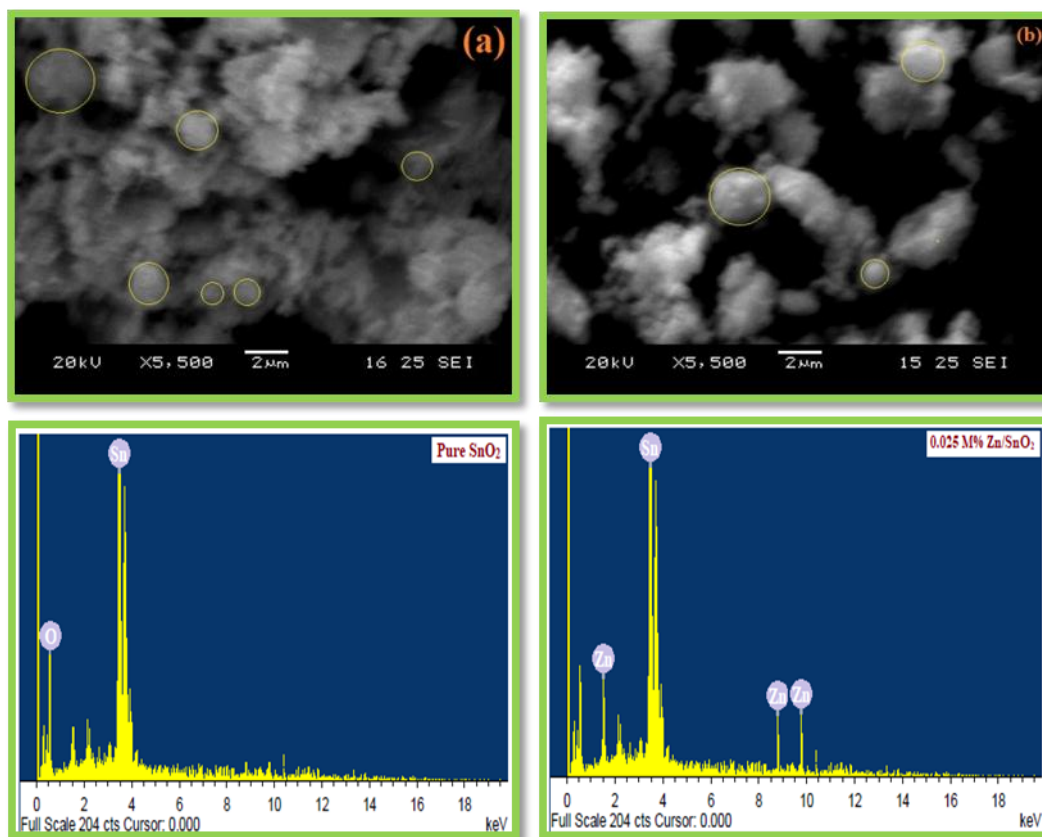
Figure 2. SEM images of samples (a) SnO_2 nanoparticles, (b) 0.025 M% Zn/ SnO_2 spherical nanoparticles.

As depicted in Fig. 2 (a, b), the undoped SnO_2 nanoparticles product exhibits the spherical particles by the presence of little agglomeration, whereas, the 0.025M% Zn/SnO_2 products are depicted the spherical particles are presented with a high degree of agglomeration. The agglomeration can be expected to the non-uniform dispersion from Zn into the SnO_2 lattice. In order, to the doped product was confirming the morphology, HR-TEM measurement was made Particle size is estimated at about 12.5 - 22.5 nm is using XRD. The agglomeration is increased when the particle size moves towards the nanoscale. The compositions of Zn/SnO_2 were investigated by EDX as depicted on the Fig.2. Nanomaterials were collected from three elements, O, Zn and Sn. This indicates the Zn atom is correctly inserted in Zn/SnO_2 properly [18].

HR-TEM and SAED patterns are undoped and 0.025% Zn/SnO_2 doped nanoparticles are appearing in Fig.3. It can be watched when the agglomerates are formed in a superposition of particles of nanometric size. Atomic planes can also be clearly observed from HR-TEM pictures. The TEM image depicts that the undoped particle size of SnO_2, which is annealed at 700°C, is less than 22.5 nm. In any case, for 0.025 % of Zn/SnO_2 powder, the particle size 12.5 nm is slightly less than of the undoped SnO_2 particles. It is potential to conclude that Zn doping can clearly assist in the production nanosized SnO_2 particles. These perceptions affirm the small size of SnO_2 nanoparticles and the acquired values are in great concurrence with the size of crystallites computed from the Scherrer condition [19]. Fig 3 (d) (h) depicts its selected area electron diffraction (SAED) pattern. Clearly that the powders have crystallized in the rutile phase. This tetragonal pattern depicts the sample is high crystallinity. The graphical size distribution histogram presented in Fig.3, which is obtained from the micrograph from the image of undoped and Zn (0.025%) doped SnO_2 nanoparticles and get in average particle size is 22.5 nm and 12.5 nm respectively with the help of image J viewer Software.
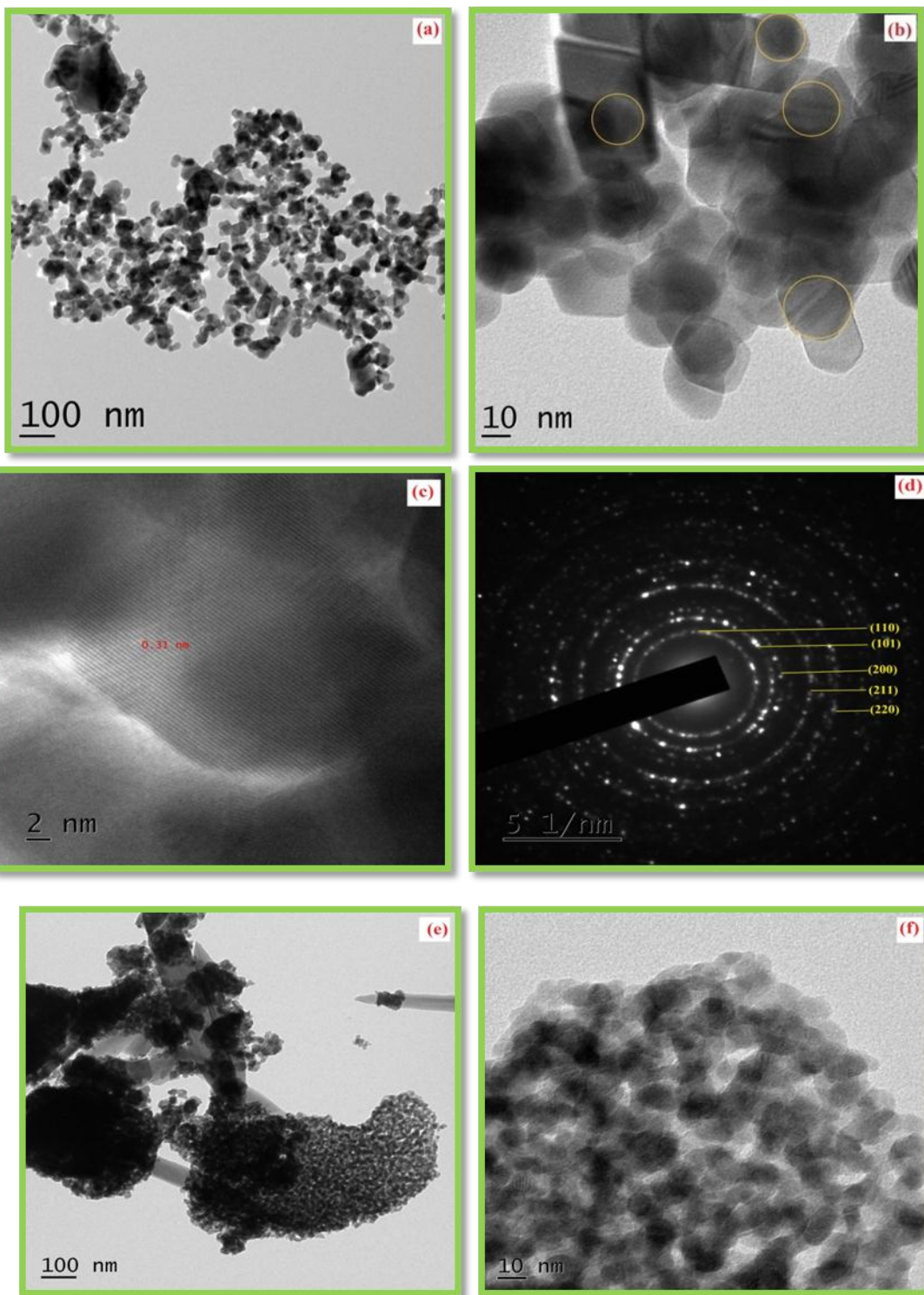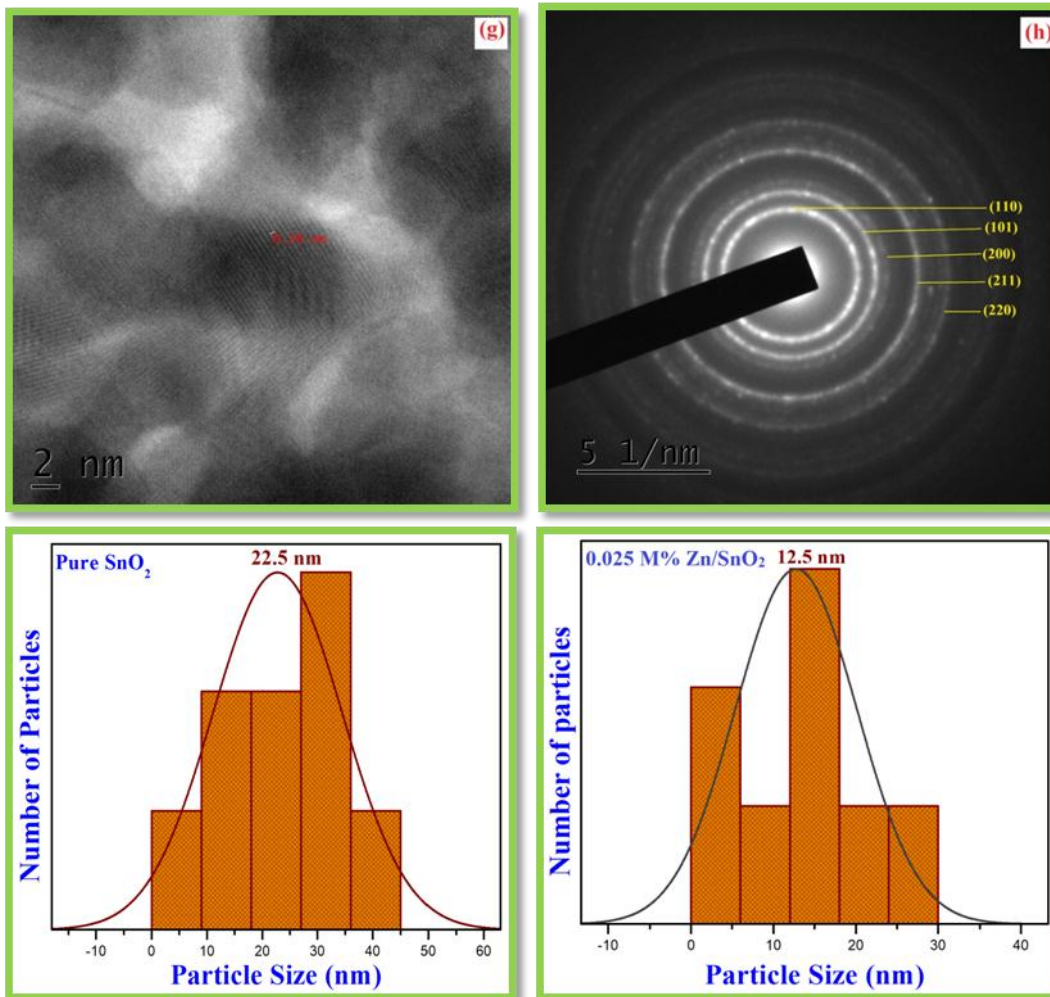
Figure 3. HR-TEM images and corresponding SAED patterns of undoped (a, b, c, d) and 0.025 M % Zn doped (e, f, g, h) SnO$_2$ nanoparticles and histogram.
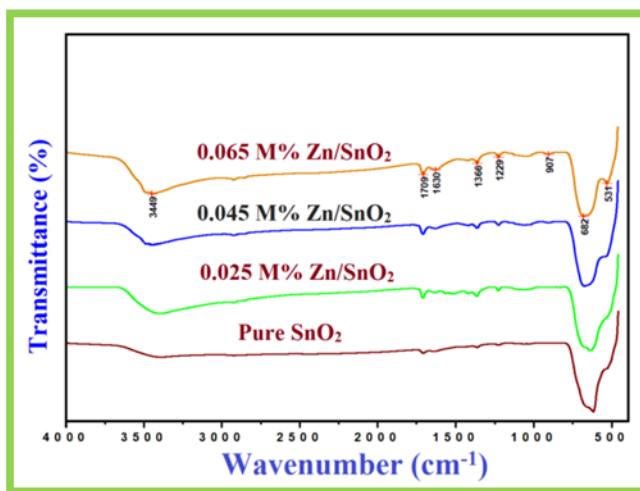
C. Functional Group Analysis

Figure 4. FTIR spectrum of SnO$_2$ nanoparticles with different Zinc concentrations.

       6

FTIR is a more sensitive technique as compared to the XRD characterization of phases and lattice distortions. Fig.4 depicts the FTIR spectra recorded in the range 400 cm^{-1} to 4000 cm^{-1} in order to confirm the phase purity of Zn/SnO$_2$ nanoparticles annealed at 700°C. The observed broad peak at 531 cm^{-1} to 682 cm^{-1} range is due to possible vibrations of Sn-O and O-Sn-O modes [20]. The peak in 1229, 1366, 1630 and 1709 cm^{-1} are due to possible vibrations of Sn-OH and H$_2$O modes [20] The broad peak at 3449 cm^{-1} and 3000 cm^{-1} is due to the possible vibrations of Sn-OH mode. [21] The absorption peaks of CO$_2$ mode assigned between 2300 -3000 cm^{-1} [22]. The enhancement in band intensity and bandwidth indicates a reduction in particle size. [23] So the size of the particles annealed at 700°C. The FTIR analysis strongly supports XRD and TEM analyses.

D. UV-DRS studies

Optical property of a metal oxide semiconductor material is the key of one parameter deciding its photoluminescence performance, which makes crucial the assurance of the optical band gap Fig.5 shows the UV-Vis diffuse reflectance spectra of the undoped and (0.025, 0.045, 0.065 M %) Zn/SnO$_2$ nanoparticles. All spectrums depict the intense absorption in the recorded wavelength range 200-700 nm.
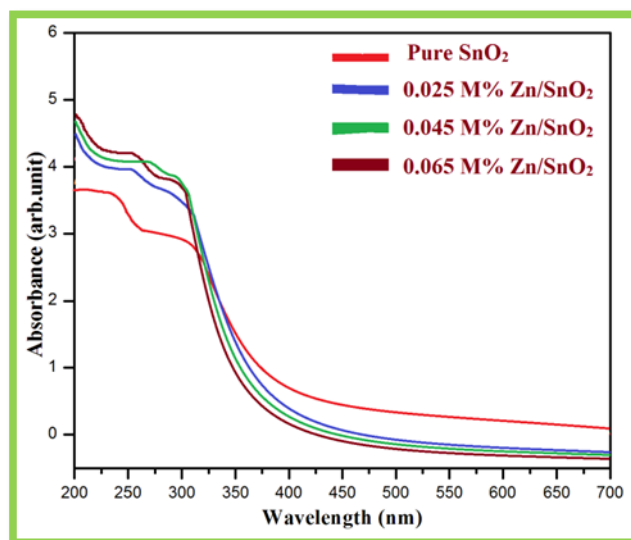

Figure 5. UV-vis DRS of undoped and Zn/SnO$_2$ nanoparticles absorbance spectra.
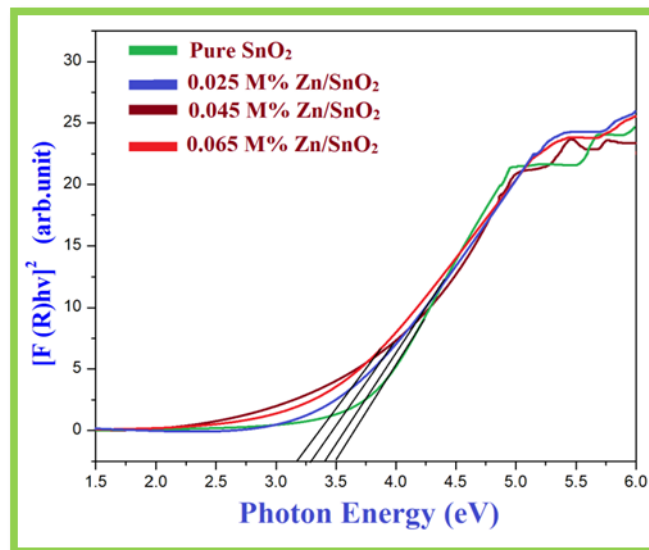

Figure 6. Band gap evaluation from the plots of (A$h\upsilon$)^2 versus Photon energy ($h\upsilon$) of undoped doped and Zn/SnO$_2$ nanoparticles.

The inception of the absorption bands, displays a red-shift when the doping concentration increments from 0.000 to 0.065 at %. To obtain more quantitative insight in the optical properties as the function of Zn content, the band gap energy value (Eg), for every Zn/SnO$_2$ nanopowders was predictable for the intersection point of the line tangent of the Tauc's curve inflection point with the horizontal energy axis (Fig.6) utilizing the following Tauc's plot formula [24] behind assuming that cassiterite SnO$_2$ was a direct bandgap semiconductor [25].

$$(\alpha \, (h\nu))^2 = A \, (h\nu - Eg)$$

Where α is the absorption coefficient (or optical density), Eg stands for band gap energy, ν is the light frequency and A is constant. The band gap energy values then changed from 3.50 eV for undoped SnO$_2$ to 3.20 eV for 0.065 M% Zn/SnO$_2$, the electromagnetic spectrum is corresponding to the near ultraviolet-violet region. Thusly, the increase in the Zinc doping concentration brings on liberal decreases of the band gap value. This was ascribed to the part of a secondary phase ZnO [26]. Still, no confirmation of the arrangement of ZnO was found in the case of Zn/SnO$_2$ nanopowders prepared by the chemical precipitation route. Therefore, the less energy band gap of the values can more probable ascribe to the melting of an impurity band into the conduction band, hence the decreasing bandwidth and the occurrence of Zn^{2+} in the Sn^{4+} in the cation sites. Hence Zn^{2+} was really integrated in the system and determined the semiconducting properties of the material [27] which is completely steady with the literature data described for doped SnO$_2$ nanopowders [28,29] Regardless, the magnitude of the red shift observed with Zinc as dopant is much less pronounced than that observed with before transition metal ions as cobalt (Co) or vanadium (V) where the energy gap decrease was rationalized based on s-d and p-d exchange interactions among the band electrons of SnO$_2$ and the localized d electrons of the transition metal ions substituting Sn^{4+} ions [30,31]. At the last moment, these results are find out the new pathways in photoluminescence, which is the modifications of Zinc content led to a fine tuning of the optical absorption of these materials.

E. Photoluminescence Studies

At the Room temperature PL emission spectra are excited at the wavelength of 251 nm of Zn/SnO$_2$ nanoparticles with the different concentrations of Zn is recorded. As show in Fig.7, each nanoparticle has a similar peak at around 326 nm. Prepared SnO$_2$ nanoparticles additionally distinguish a PL peak at around 326 nm [32]. At the point when the Zn concentration increased to 0.025at %, the two new broad peaks at around 353 nm and 368 nm are observed. Additionally, increasing the Zinc concentration to 0.065 M%, the intensity of these new peaks is increased.
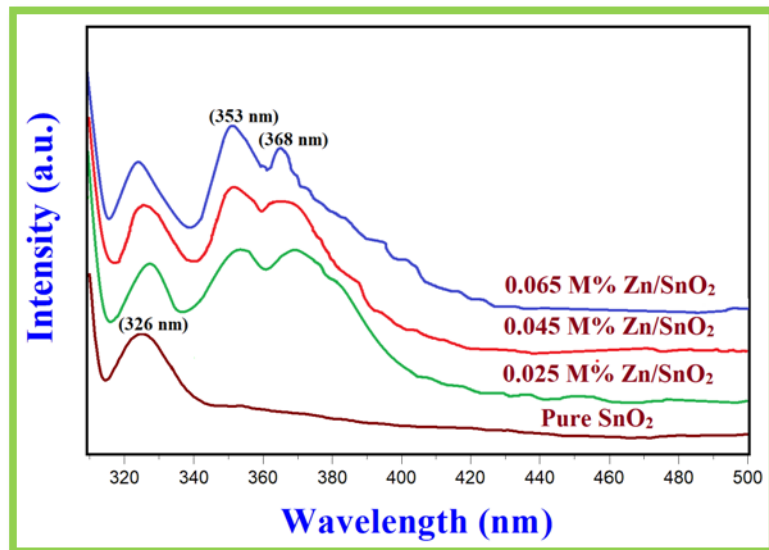

Figure 7. PL spectrum of undoped and Zn/SnO$_2$ nanoparticles.

Generally, oxygen vacancies are the normal defects in the metallic oxides which further go in luminescent procedures at the center of the radioactive [33]. They are three different charge state were occurring in the oxygen vacancies that are V_0^0, V_0^+ and V_0^{2+} [34]. Among these charged states, V_0^0 is a shallow benefactor, which lies almost to the conduction band. It is

believed that most of the oxygen vacancies are likely in the V_0^{2+} state [35]. Since ionic radius of Zn^{2+} (0.074 nm) with Sn^{4+} (0.069 nm) are equivalent, Zn can simply substitute for Sn^{4+} in host lattice. The lack V_0^{2+} charge can be seen as an oxygen vacancy. As it were, the incorporation of Zn^{2+} into SnO_2 lattice can make oxygen vacancy V_0^{2+}. As a result, two novel new peaks in PL medium around 351 - 369 nm are showed because of Zn doped. In general, the PL medium observed red shift could be attributed. It has been accounted that the PL spectra at the red shift can be attributed to the effect of compressive stress [36, 37]. Even though Zn/SnO_2 nanoparticles are in a tensile stress state (c<co), Zn^{2+} ions compared with Sn^{4+} ions, which subsides the impact of tensile stress state in films [38]. So the progressions of the PL spectra with the different concentration of Zn propose that the defects and stress influenced by Zn doping assume a vital part in the photoluminescence behavior.

F. Electrochemical Properties Analysis

The CV measurements were made in investigating electrochemical performances. Although the compound electrochemical efficiency of cyclic voltammetry measured the potential window between -1.6 and 1.5 mV/s shows in Fig.8. The undoped and Zn/SnO_2 nanoparticles were tested as the electrode to evaluate the improved electrochemical performance in a three electrode system. It exhibits Quasi Rectangular Shape of the cyclic voltammetry curve with scan rate 5-100 mV/s. The specific capacitances were synthesized by undoped and Zn/SnO_2 nanoparticles can be calculated by using this formula [39, 40].

$$Cs = \frac{Q}{\Delta v \cdot m}$$

Here, Cs stands for the specific capacitance, Q for anode charge and m is the mass of the prepared electrode material and Δv scan rate. The estimate of electrochemical is completed at 0.2 M $C_{16}H_{36}ClNO_4$ with a standard three electrode designs comprising of a sample working electrode, an Ag/AgCl is reference electrode and a platinum wire is counter electrode [41]. Table.2 shows the specific capacitance value of undoped and Zn/SnO_2 nanoparticles. A specific capacitance value of 497 F/g and 572 F/g was obtained for the undoped and (0.025%) Zn/SnO_2 nanoparticles at a lower scan rate of 5 mV/s. The capacitance value is high which is due to the high crystallinity of the product and the zinc doping, as well as the porous morphology [42], confirmed by XRD and TEM. The mobility of the charge carriers and the crystallinity of the products increased due to zinc doping as well as increase the capacitance. The obtained capacitance values of SnO_2 synthesized by other wet chemical techniques were higher than reported values [43]. The changes in specific capacitance while raising the scan rate owing to the pseudocapacitance nature of the undoped and Zn/SnO_2 nanoparticles. A faradic reaction, it indicates that the lower scan rate in the ionic diffusion happens only in the inner (core) and an outer surface of the material. Whereas, increase the scan rate in the ionic diffusion it happens just only the outer surface of the nanoparticles [44]. From the cyclic voltammetry study, the reduction peaks are appearing at 0.4 and 0.8 V and oxidation peak at 0.7 V was obtained. When scan rate increases the curve also changed which is represented good capacitance performance and good reversibility of Zn/SnO_2 nanoparticles. The Zn/SnO_2 nanoparticles is annealed at 700^oC with high specific capacitance value of 572 F/g this gives a better report than previous work Co_2SnO_4/activated carbon was specific capacitance value 285 F/g by sol–gel route [45]. The scan rate increases with a capacitance values decrease, which is the behavior of electrochemical systems. The most important factors influencing the entire specific capacitances difference with scan rate are: (i) the increase scan rate with decreasing in specific capacitances was assigned to the reduced diffusion rate of the ions in the pores at higher scan rates. The increase in scan rate directly reduced the ion diffusion, since at high scan rates the ions approach only the outer surface of the electrode material. (ii) The surface adsorption process at high scan rates. This is based on the diffusion effects of the proton within the electrode material. Hence, it is held that part of the surface of the electrode materials contributes to a high charging/discharging rate, which decreased the specific capacitance at higher scan rates [46].
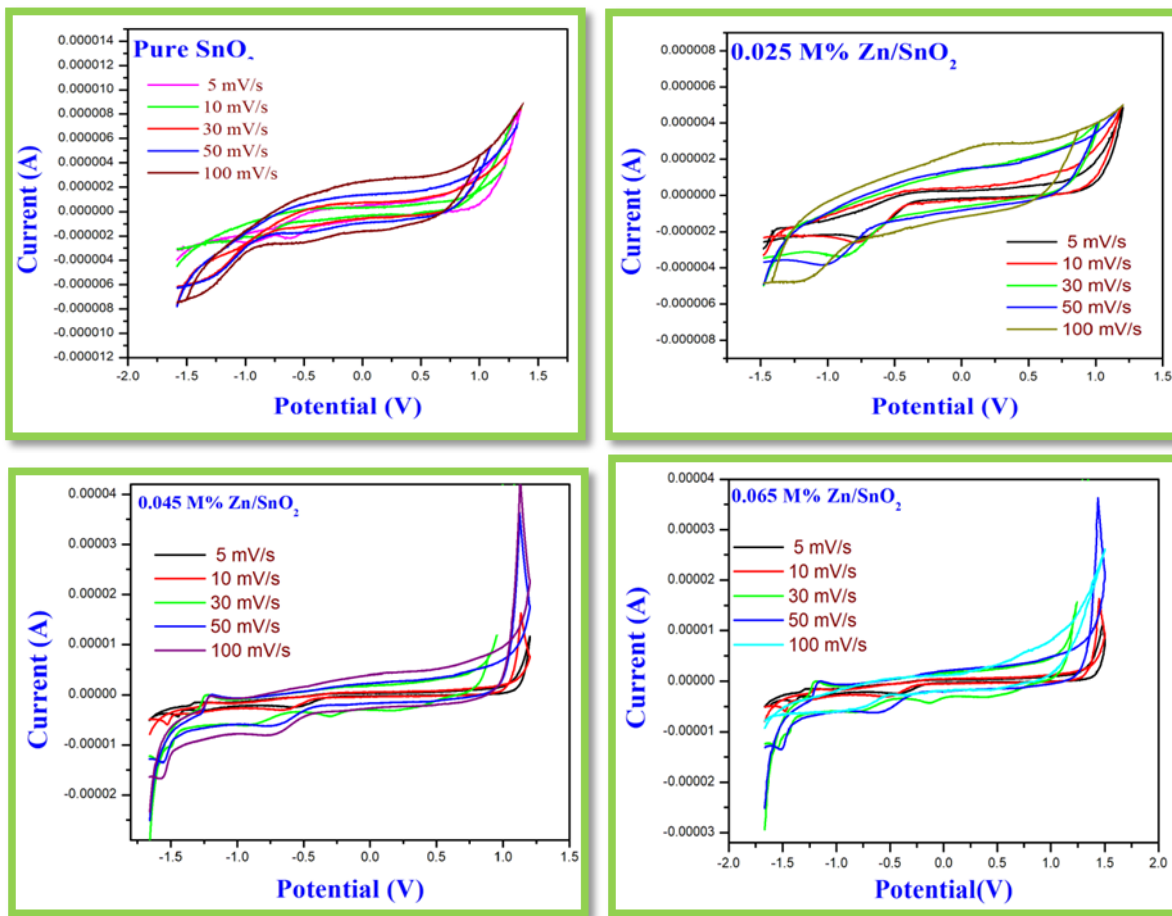
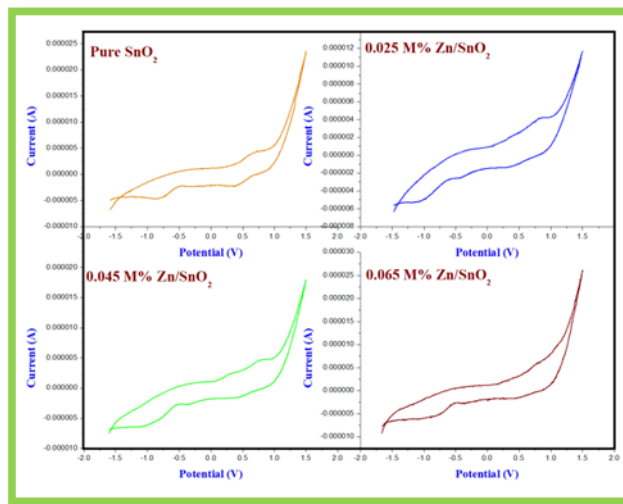Figure 8. CV curve of specific capacitance on Undoped and Zn/SnO$_2$ nanoparticles.

Figure 8 (a). CV curve of specific capacitance on high scan rate of undoped and Zn/SnO$_2$ nanoparticles.
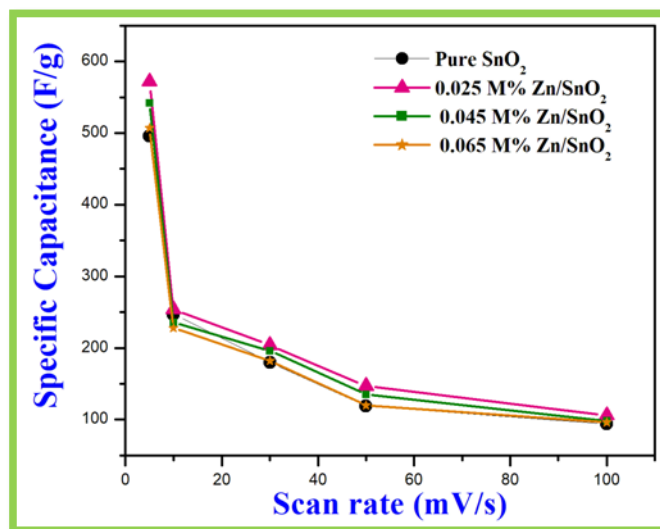
Figure 8 (b). Dependence of specific capacitance as a function of scan rate of undoped and Zn/SnO_2 nanoparticles.

Table.2. The different scan rate and their specific capacitance value of pure and Zn/SnO_2
(0.025%, 0.045%, 0.065%) annealed at 700°C.

Scan Rate (mVs^{-1})	Specific Capacitance (Fg^{-1})			
	Pure SnO_2	Zn/SnO_2 (0.025%)	Zn/SnO_2 (0.045%)	Zn/SnO_2 (0.065%)
5	496	572	542	507
10	247	254	236	228
30	180	204	196	182
50	119	147	135	120
100	94	106	98	96

IV. CONCLUSIONS

Undoped and (0.025, 0.045, 0.065 M %) Zn/SnO_2 nanoparticles are synthesized via chemical precipitation route it annealed at 700^oC. The XRD analysis were confirmed the undoped and 0.025 M % Zn/SnO_2 nanoparticles is tetragonal structure and secondary phase of the hexagonal is ZnO was distinguished at 0.045 and 0.065 M % Zn/SnO_2 nanoparticles, the average crystallite size ranges from 11.6 to 42.0 nm. SEM studied the synthesized product with an agglomerated spherical shape. EDX confirmed that the prepared samples are only containing Zn, Sn, and O with no different impurities. The average grain size of a TEM picture ranges from 12.5 to 22.5 nm which concurs with the average crystallite size ~11.6 nm calculated by Scherrer's equation from XRD pattern. The observed photoluminescence of the nanocomposites is attributed to electron transfer by lattice defects and oxygen vacancies. The superior specific capacitance value of 596 F/g was gotten at the scanning rate of 5 mV/s. We believe that too easy process and specific capacitance performance also clears a way to prepare stable 0.025% Zn/SnO_2 nanoparticles, which is predictable survive a potential possibility for supercapacitor applications.

Disclosure of interest
The authors declare that they have no conflicts of interest concerning this article.

REFERENCES

[1] B. E. Conway, "*Electrochemical supercapacitors: scientific fundamentals and technological applications*". Springer Science & Business Media, 2013.

[2] D. Bélanger, X. Ren, J. Davey, F. Uribe, Shimshon Gottesfeld. "*Characterization and long‑term performance of polyaniline‑based electrochemical capacitors*," Journal of theElectrochemicalSociety, Vol.**147**, No.**8**, pp.**2923-2929, 2000.** https://doi.org/10.1149/1.1393626

[3] F.Fusalba, P. Gouérec, D. Villers, and D. Bélanger, "*Electrochemical characterization of polyaniline in nonaqueous electrolyte and its evaluation as electrode material for electrochemical supercapacitors,*" Journal of the Electrochemical Society, Vol.**148**, No.**1** pp.**A1-A6, 2001**. https://doi.org/10.1149/1.1339036

[4] J. P. Zheng, P. J. Cygan, T. R. Jow, "*Hydrous ruthenium oxide as an electrode material for electrochemical capacitors,*" Journal of the Electrochemical Society Vol.**142**, No.**8**, pp.**2699-2703**, **1995**. https://doi.org/10.1149/1.2043984

[5] J. K. Chang, W. T. Tsai, "*Material characterization and electrochemical performance of hydrous manganese oxide electrodes for use in electrochemical pseudocapacitors,*" Journal of the Electrochemical Society, Vol.**150**, No.**10,** pp.**A1333-A1338, 2003**. https://doi.org/10.1149/1.1605744

[6] Kim,Il-Hwan, K. B. Kim, "*Ruthenium oxide thin film electrodes for supercapacitors,*" Electrochemical and Solid-State Letters, Vol.**4**, No.**5** pp.**A62-A64**, **2001**. https://doi.org/10.1149/1.1359956

[7] H. C. Chiu, C. S. Yeh, "*Hydrothermal synthesis of SnO2 nanoparticles and their gas-sensing of alcohol,*" The Journal of Physical Chemistry C, Vol.**111**, No.**20**, pp.**7256-7259, 2007**. https://doi.org/10.1021/jp0688355

[8] D. N. Srivastava, S. Chappel, O. Palchik, A. Zaban, A. Gedanken, "*Sonochemical synthesis of mesoporous tin oxide,*" Langmuir Vol.**18**, No.**10**, pp.**4160-4164**, **2002**. https://doi.org/10.1021/la015761+

[9] J. Zhu, Z. Lu, S. T. Aruna, D. Aurbach, A. Gedanken. "*Sonochemical synthesis of SnO2 nanoparticles and their preliminary study as Li insertion electrodes,*" Chemistry of Materials, Vol.**12**, No.**9**, pp.**2557-2566**, **2000**. https://doi.org/10.1021/cm990683l

[10] H. Jin, Y. Xu, G. Pang, W. Dong, Q. Wan, Y. Sun, S. Feng, "*Al-doped SnO2 nanocrystals from hydrothermal systems,*" Materials chemistry and physics, Vol.**85**, No.**1**, pp.**58-62**, **2004**. https://doi.org/10.1016/j.matchemphys.2003.12.006

[11] J. Hays, A. Punnoose, R. Baldner, Mark H. Engelhard, J. Peloquin, K. M. Reddy, "*Relationship between the structural and magnetic properties of Co-doped SnO2 nanoparticles,*" Physical Review B, Vol.**72**, No.**7**, pp.**075203**, **2005**. https://doi.org/10.1103/PhysRevB.72.075203.

[12] Wu, Nae-Lih, "*Nanocrystalline oxide supercapacitors,*" Materials Chemistry and Physics, Vol.**75**, No.**1-3**, pp.**6-11, 2002**. https://doi.org/10.1016/S0254-0584(02)00022-6

[13] A. A. Ismail, A. El-Midany, E. A. Abdel-Aal, H. El-Shall, "*Application of statistical design to optimize the preparation of ZnO nanoparticles via hydrothermal technique.*" Materials Letters, Vol.**59**, No.**14-15**, pp.**1924-1928, 2005**. https://doi.org/10.1016/j.matlet.2005.02.027

[14] M. M. Rashad, A. A. Ismail, I. Osama, I. A. Ibrahim, Abdel-Hakim T. Kandil. "*Photocatalytic decomposition of dyes using ZnO doped SnO2 nanoparticles prepared by solvothermal method,*" Arabian Journal of Chemistry, Vol.**7**, No.**1,** pp.**71-77**, **2014**. https://doi.org/10.1016/j.arabjc.2013.08.016

[15] A. Enesca, L. Andronic, A. Duta, "*Optimization of opto-electrical and photocatalytic properties of SnO2 thin films using Zn^{2+} and W^{6+} dopant ions.*" Catalysis letters, Vol.**142**, No.**2**, pp.**224-230**, 2012. https://doi.org/10.1007/s10562-011-0762-4

[16] A. L. Patterson, "*The Scherrer formula for X-ray particle size determination,*" Physical review, Vol.**56**, No.**10,** pp.**978**, **1939**. **https://doi.org/10.1103/PhysRev.56.978**.

[17] J.Wang, H. Fan, H. Yu, "*Synthesis of Hierarchical Porous Zn-Doped SnO2 Spheres and Their Photocatalytic Properties,*" Journal of Materials Engineering and Performance, Vol.**24**, No.**11**, pp.**4260-4266**, **2015**. https://doi.org/10.1007/s11665-015-1745-1

[18] Sagadevan, Suresh, J. Podder. "*Investigation on structural, surface morphological and dielectric properties of Zn-doped SnO2 nanoparticles,*" Materials Research, Vol.**19**, No.**2** pp.420-**425**, **2016**. http://dx.doi.org/10.1590/1980-5373-MR-2015-0657

[19] R. Bargougui, A. Oueslati, G. Schmerber, C. Ulhaq-Bouillet, S. Colis, F. Hlel, S. Ammar, A. Dinia, "*Structural, optical and electrical properties of Zn-doped SnO2 nanoparticles synthesized by the co-precipitation technique,*" Journal of Materials Science: Materials in Electronics, Vol.**25**, No.**5**, pp.**2066-2071**, 2014. https://doi.org/10.1007/s10854-014-1841-2

[20] D.Amalric-Popescu, F. Bozon-Verduraz, "*Infrared studies on SnO2 and Pd/SnO2,*" Catalysis today, Vol.**70**, No.**1-3**, pp.**139-154**, **2001**. https://doi.org/10.1016/S0920-5861(01)00414-X

[21] S. Zulfiqar, Z. Iqbal, Jianguo Lü, "*Zn–Cu-codoped SnO2 nanoparticles: Structural, optical, and ferromagnetic behaviors,*" Chinese Physics B, Vol.**26**, No.**12**, pp.**126104**, **2017**. https://doi.org/10.1088/1674-1056/26/12/126104

[22] S. Mehraj, M. Shahnawaze Ansari, "*Rutile-type Co doped SnO2 diluted magnetic semiconductor nanoparticles: structural, dielectric and ferromagnetic behavior,*" Physica B: Condensed Matter, Vol.**430**, pp.**106-113**, **2013**. https://doi.org/10.1016/j.physb.2013.08.024

[23] Y. Yuan, Q. Jiang, J. Yang, L. Feng, W. Wang, Z. Ye, J. Lu, "*Variation in luminescence and bandgap of Zn-doped SnO2 nanoparticles with thermal decomposition,*" Journal of Materials Science: Materials in Electronics, Vol.**27**, No.**9** pp.**9541-9549**, **2016**. **https://doi.org/10.1007/s10854-016-5006-3**

[24] E. A. Davis, NFf Mott, "*Conduction in non-crystalline systems V. Conductivity, optical absorption and photoconductivity in amorphous semiconductors,*" Philosophical Magazine, Vol.**22**, No.**179** pp.0903-**0922**, **1970.** https://doi.org/10.1080/14786437008221061

[25] G. Yang, Z. Yan, T. Xiao, "*Preparation and characterization of SnO2/ZnO/TiO2 composite semiconductor with enhanced photocatalytic activity*" Applied surface science, Vol.**258**, No.**22** pp.8704-**8712**, **2012**. https://doi.org/10.1016/j.apsusc.2012.05.078

[26] N. Shanmugam, T. Sathya, G. Viruthagiri, C. Kalyanasundaram, R. Gobi, and S. Ragupathy, "*Photocatalytic degradation of brilliant green using undoped and Zn doped SnO2 nanoparticles under sunlight irradiation,*" Applied Surface Science, Vol.**360,** pp.**283-290**, **2016.** https://doi.org/10.1016/j.apsusc.2015.11.008

[27] A.Sharma, M. Varshney, S. Kumar, K. D. Verma, Ravi Kumar, *"Magnetic properties of Fe and Ni doped SnO₂ nanoparticles,"* Nanomaterials and Nanotechnology, Vol.**1**, pp.**29-33**, **2011**. https://doi.org/10.5772/50948

[28] S.Nilavazhagan, S. Muthukumaran, M. Ashokkumar. *"Cu-doping effect on the structural, optical and photoluminescence properties of Sn₀.₉₈Cr₀.₀₂O₂ nanoparticles by co-precipitation method,"* Journal of Materials Science: Materials in Electronics, Vol.**24**, No. **7**, pp.**2581-2592**, **2013**. https://doi.org/10.1007/s10854-013-1137-y

[29] B. Xu, X. G. Ren, G. R. Gu, L. L. Lan, B. J. Wu, *"Structural and optical properties of Zn-doped SnO₂ films prepared by DC and RF magnetron co-sputtering"* Superlattices and Microstructures, Vol.**89**, pp.**34-42**, **2016**. https://doi.org/10.1016/j.spmi.2015.10.043

[30] W. B.Soltan, M. Mbarki, S. Ammar, O. Babot, T. Toupance, *"Structural and optical properties of vanadium doped SnO₂ nanoparticles synthesized by the polyol method,"* Optical Materials. Vol.**54**, pp.**139-146, 2016**. https://doi.org/10.1016/j.optmat.2016.01.059

[31] S.Ghosh, D. De Munshi, K. Mandal, *"Paramagnetism in single-phase Sn₁₋ₓCoₓO₂ dilute magnetic semiconductors,"* Journal of Applied Physics, Vol.**107**, No.**12** pp.123919, **2010**. https://doi.org/10.1063/1.3437641

[32] S. Luo, J. Fan, W. Liu, M. Zhang, Z. Song, C. Lin, X. Wu, P. K. Chu, *"Synthesis and low-temperature photoluminescence properties of SnO₂ nanowires and nanobelts,"* Nanotechnology, Vol.**17**, No.**6**, pp.**1695**, **2006**. https://doi.org/10.1088/0957-4484/17/6/025

[33] L. Z. Liu, X. L. Wu, J. Q. Xu, T. H. Li, J. C. Shen, P. K. Chu, *"Oxygen-vacancy and depth-dependent violet double-peak photoluminescence from ultrathin cuboid SnO₂ nanocrystals,"* Applied Physics Letters, Vol.**100**, No.**12** pp.**121903, 2012.** https://doi.org/10.1063/1.3696044

[34] K. Vanheusden, W. L. Warren, C. H. Seager, D. R. Tallant, J. A. Voigt, B. E. Gnade, *"Mechanisms behind green photoluminescence in ZnO phosphor powders,"* Journal of Applied Physics, Vol.**79**, No.**10**, pp.**7983-7990**, **1996**. https://doi.org/10.1063/1.362349

[35] P. S. Shajira, M. Junaid Bushiri, Bini B. Nair, V. Ganeshchandra Prabhu, *"Energy band structure investigation of blue and green light emitting Mg doped SnO₂ nanostructures synthesized by combustion method."* Journal of Luminescence, Vol.**145**, pp.**425-429**, **2014**. https://doi.org/10.1016/j.jlumin.2013.07.073

[36] J. Ni, X. Zhao, X. Zheng, J. Zhao, B. Liu, *"Electrical, structural, photoluminescence and optical properties of p-type conducting, antimony-doped SnO₂ thin films,"* Acta Materialia, Vol.**57**, No.**1**, pp.**278-285**, **2009**. https://doi.org/10.1016/j.actamat.2008.09.013

[37] L.Ding, Andy Eu-Jin Lim, Jason Tsung-Yang Liow, M. B. Yu, G-Q. Lo, *"Dependences of photoluminescence from P-implanted epitaxial Ge,"* Optics Express, Vol.**20**, No.**8**, pp.**8228-8239**, **2012.** https://doi.org/10.1364/OE.20.008228

[38] T. Ungár, *"Microstructural parameters from X-ray diffraction peak broadening,"* Scripta Materialia, Vol.**51**, No.**8,** pp.**777-781**, **2004**. https://doi.org/10.1016/j.scriptamat.2004.05.007

[39] G. Y. Zhao, C. L. Xu, H. L. Li, *"Highly ordered cobalt-manganese oxide (CMO) nanowire array thin film on Ti/Si substrate as an electrode for electrochemical capacitor,"* Journal of power sources, Vol.**163**, No.**2** pp.**1132-1136**, **2007**. https://doi.org/10.1016/j.jpowsour.2006.09.085

[40] Ramachandran, Rajendran, Sathiyanathan Felix, G. M. Joshi, Bala PC Raghupathy, S. K. Jeong, A. N. Grace, *"Synthesis of graphene platelets by chemical and electrochemical route,"* Materials Research Bulletin, Vol.**48**, No.**10** pp.**3834-3842**, **2013**. https://doi.org/10.1016/j.materresbull.2013.05.085

[41] S. C. Pang, B. H. Wee, S. F. Chin, *"The capacitive behaviors of manganese dioxide thin-film electrochemical capacitor prototypes,"* International Journal of Electrochemistry, Vol.**2**, pp.**1–10**, **2011**. http://dx.doi.org/10.4061/2011/397685

[42] D.Deng, J. Y. Lee, *"Hollow core–shell mesospheres of crystalline SnO2 nanoparticle aggregates for high capacity Li+ ion storage,"* Chemistry of Materials, Vol.**20**, No.**5** pp.**1841-1846**, **2008**. https://doi.org/10.1021/cm7030575

[43] K. R. Prasad, N. Miura, *"Electrochemical synthesis and characterization of nanostructured tin oxide for electrochemical redox supercapacitors,"* Electrochemistry communications, Vol.**6**, No.**8**, pp.**849-852, 2004**. https://doi.org/10.1016/j.elecom.2004.06.009

[44] P.Sivagurunathan, S. R. Gibin, *"Preparation and characterization of nickel ferrite nanoparticles by co-precipitation method with citrate as chelating agent,"* Journal of Materials Science: Materials in Electronics, Vol.**27**, No.3 pp.**2601-2607**, **2016.** https://doi.org/10.1007/s10854-015-4065-1

[45] P.He, Z. Xie, Y. Chen, F. Dong, H. Liu. *"Co₂SnO₄/activated carbon composite electrode for supercapacitor,"* Materials Chemistry and Physics, Vol.**137**, No.**2** pp.**576-579**, **2012.** https://doi.org/10.1016/j.matchemphys.2012.10.004

[46] R. K. Selvan, I. Perelshtein, N. Perkas, Aharon Gedanken, *"Synthesis of hexagonal-shaped SnO2 nanocrystals and SnO2@ C nanocomposites for electrochemical redox supercapacitors."* The Journal of Physical Chemistry C Vol.**112**, No.**6** pp.**1825-1830**, **2008**. **https://doi.org/10.1021/jp076995q**

AUTHORS PROFILE

Dr. S. Sivakumar M.Sc., B.Ed., M.Phil., Ph.D. is currently working as Assistant professor (SG) Department of Physics Annamalai University, Annamalainagar 608002. He has published more than 45 research papers in reputed international journals, conferences, and Elsevier journals and it's also available online. His main research work focuses on Spectroscopy, biophysics and materials science (nanoscience) based education. He has 18 years of teaching experience and 12 years of research experience. *E-mail:* girihari777@yahoo.com

Mr. E. Manikandan M.Sc., He is studying on Ph.D., Research Scholar (2015-18), Department of Physics, Annamalai University, Annamalainagar. He is working on research area of "Nanoscience and Application". *E-mail:* e.mani16041992@gmail.com